
Volume 307, Issues 3–4
15 July 2011
ISSN 0012-821X
ELSEVIER
EARTH
& PLANETARY
SCIENCE LETTERS
Editors
Rick Carlson, Washington, DC
Peter B. deMenocal, Palisades, NY
T. Mark Harrison, Los Angeles, CA
Gideon M. Henderson, Oxford, UK
Yanick Ricard, Lyon
P. Shearer, La Jolla, CA
Tilman Spohn, Berlin
Lars Stixrude, London

Earth and Planetary Science Letters 307 (2011) 369–376

Contents lists available at ScienceDirect

Earth and Planetary Science Letters

journal homepage: www.elsevier.com/locate/epsl

Anisotropy as cause for polarity reversals of D″ reflections

Christine Thomas [a,*], James Wookey [b], John Brodholt [c], Thomas Fieseler [a]

[a] Institut für Geophysik, Westfälische Wilhelms Universität Münster, Corrensstr 24, 48149 Münster, Germany
[b] School of Earth Sciences, University of Bristol, Wills Memorial Building, Queen's Road, Bristol, BS8 1RJ, UK
[c] Department of Earth Sciences, University College London, Gower Street, London WC1E 6BT, UK

ARTICLE INFO

Article history:
Received 28 December 2010
Received in revised form 4 May 2011
Accepted 6 May 2011
Available online 31 May 2011

Editor: P. Shearer

Keywords:
lower mantle
polarity
anisotropy
post-perovskite

ABSTRACT

Recordings of seismic events that sample the deep mantle can test different hypotheses of mantle processes and composition. Seismic reflections from structures in the D″ region — the bottom 200–400 km of the Earth's mantle — can provide information on the velocity contrasts in this region. By studying the waveforms and polarities of the D″ reflections in P and S-waves, we can potentially distinguish between different explanations for the observed structures, such as phase transitions, mineral texture or thermal anomalies. Here we use source–receiver combinations that contain reflections from D″ in two different regions that are both characterised by fast seismic velocities in tomographic models. Beneath the Caribbean a positive S-velocity contrast but negative P-wave velocity contrast across the D″ reflector has been reported previously, consistent with a model of a phase change in $MgSiO_3$. In the second fast velocity region (Eurasia) we detect positive P- and S-wave velocity contrasts in two orthogonal paths crossing in the lowermost mantle indicating a different scenario for D″. A path that crosses this region in 45° to the other two great circle paths shows evidence for a negative P velocity contrast. One explanation to reconcile observations in both regions is a phase transition from perovskite to post-perovskite with a fraction of 12% preferred crystal alignment in the post-perovskite phase. Depending on the travel direction of the waves with respect to the flow direction in the lower mantle, positive or negative velocity jumps can be expected. Other anisotropic models are considered but cannot fully explain the range of observations we find in the data.

1. Introduction

The lowermost Earth's mantle (the D″ region Bullen, 1949) exhibits a large number of variable seismic structures. These structures range from small-scale scatterers near the core–mantle boundary (CMB) to several hundred kilometres above the CMB (e.g. Hedlin et al., 1997; Thomas et al., 1999; Vidale and Hedlin, 1998), and ultra-low velocity zone (ulvz, e.g., Garnero et al., 1998; Rost and Revenaugh, 2003) to large-scale reflectors in regions of possible palaeo-subduction (Lay and Helmberger, 1983; Wysession et al., 1998 for a review). Recently, large-scale reflectors have also been found in regions where tomographic inversions (e.g., Grand, 2002; Kárason and van der Hilst, 2001; Masters et al., 2000) find large low-velocity regions (e.g. Lay et al., 2006; Ohta et al., 2008). In several regions of the Earth seismic anisotropy in the lowermost mantle has been reported (e.g., Kendall and Silver, 1998; Lay et al., 1998; Rokosky et al., 2006; Wookey et al., 2005a). Especially in regions of fast seismic velocity (e.g. Grand, 2002) a case of vertical transverse isotropy (VTI) or tilted TI can explain the data (Garnero et al., 2004; Maupin et al., 2005; Ritsema and Van Heijst, 2000; Thomas et al., 2007; Wookey and Kendall, 2008). Regions with slow seismic velocities seem to exhibit a more complex anisotropic scenario (see, e.g., Pulliam and Sen, 1998; Kendall and Silver, 1998; Lay et al., 1998).

Waves that reflect off structures in the D″ region, such as PdP and SdS (e.g., Weber, 1993) have been used to determine the presence and extent of seismic structures in the lowest few hundred kilometres of the mantle (e.g., Kendall and Shearer, 1994; Lay and Helmberger, 1983; Weber, 1993; Wysession et al., 1998). These reflected waves arrive with a travel time and slowness between P (S) and PcP (ScS) and through the use of array seismology they can be distinguished from other arrivals (e.g., Thomas et al., 2004a, b; Weber, 1993; Weber and Davis, 1990). Recently more than one reflection has been observed in the time window between P (S) and PcP (ScS) (Hutko et al., 2006, 2008; Kawai et al., 2007; Kito et al., 2007; Lay et al., 2006; Thomas et al., 2004a, b; van der Hilst et al., 2007) indicating a more complex structure in both fast and slow velocity regions.

Several hypotheses have been advanced in recent years to explain the reflectors and anisotropy in D″, for example, subducted oceanic lithosphere and a slab graveyard at the core–mantle boundary (CMB) (e.g. Kendall, 2000) can explain seismic reflections a few hundred kilometres above the CMB as well as observations of seismic anisotropy in D″ when assuming sheared melt inclusions (Kendall and Silver, 1998). A different way to explain the reflection in D″ was proposed by Lay et al. (2004) where they invoke chemical layering at

* Corresponding author. Tel.: +49 251 83 33591; fax: +49 251 83 36100.
E-mail address: tine@earth.uni-muenster.de (C. Thomas).

0012-821X/$ – see front matter © 2011 Elsevier B.V. All rights reserved.
doi:10.1016/j.epsl.2011.05.011

the base of the mantle. Another scenario for explaining two reflectors in D″ is the model of Tan et al. (2002) where a new upwelling is generated below a subducted slab near the CMB but this model cannot explain anisotropy without invoking other mechanisms to account for it, such as sheared melt inclusions within the slab.

The recently discovered phase transition of perovskite to post perovskite (e.g. Murakami et al., 2004; Oganov and Ono, 2004; Tsuchiya et al., 2004) offers another hypothesis that can explain several seismic structures in D″. The phase transition generates a density increase (Murakami et al., 2004) but may only exhibit a small shear velocity jump (Murakami et al., 2007). Wookey et al. (2005b) used ab initio calculations to show that a small negative P-wave contrast and a positive S-wave contrast would be generated for a phase transition in $MgSiO_3$. It is also possible that the post-perovskite phase transforms back to the perovskite phase closer to the D″ region (Hernlund et al., 2005), thereby providing a mechanism to explain the two reflectors found in D″ in some fast velocity regions in the lowermost mantle (Hutko et al., 2006; Thomas et al., 2004a, b; van der Hilst et al., 2007). Recent results indicate that the post-perovskite phase is able to generate seismic anisotropy in the D″ region (e.g. Merkel et al., 2006; Oganov et al., 2005; Stackhouse and Brodholt, 2007; Yamazaki and Karato, 2007). Phase transitions to a post-perovskite phase in other minerals or in mid-ocean ridge basalts (MORB) might explain additional reflectors in D″ (Ohta et al., 2008) such as reported by Lay et al. (2006). Recently, however, Catalli et al. (2009) reported that in pyrolitic material, the phase transition to post-perovskite would take place over a large depth range, therefore not being able to produce short period P-wave reflections. Ammann et al. (2010) propose that strong crystallographic texture could be responsible for generating sharp reflectors consistent with seismic observations.

Distinguishing between the different hypotheses requires using as much information of the arriving seismic waves as possible. Waveforms and polarities of the reflections from structures in D″ provide a tool for constraining different scenarios. Here we use the polarities of reflected waves in D″ to test the hypothesis of post-perovskite anisotropy in D″ as mechanism for generating reflectors in P and S-waves.

2. Observations

Events located in South America recorded in North America have their reflection points in the D″ region beneath Central America (Fig. 1b), a region characterised by fast seismic velocities (e.g. Kárason and van der Hilst, 2001). The epicentral distances of the source–receiver combinations used for detecting reflections off structures in the D″ region are between 65 and 80°. In previous studies, Kito et al. (2007) and Hutko et al. (2008) used these event-receiver combinations and found small negative PdP waves, i.e. reflections from the top of D″. These studies and Thomas et al. (2004b) also detected positive S-wave reflections from the same region. Kito et al. (2007) and Hutko et al. (2008) used the model by Wookey et al. (2005b) that predicts small negative P-wave jumps and positive S-wave jumps for a post-perovskite phase transition in MgSiO3 and concluded that this phase transition can explain their observations. A similar scenario of positive S-wave velocity jumps and small negative P-wave velocity jumps has been detected by Chaloner et al. (2009) beneath Southeast Asia.

For a second test region we use events from the Northwest Pacific recorded in Germany with their reflection points beneath Eurasia (Fig. 1a), where tomographic models indicate fast seismic velocities in P and S-wave models (e.g. Grand, 2002; Kárason and van der Hilst, 2001). The selection criteria are the same as for the South America–North America path and the depth of the events lies between 50 and 660 km. This path has been investigated before (e.g. Thomas and Weber, 1997; Weber, 1993) and showed evidence for P- and S-wave reflections from D″ structures. For a near-perpendicular crossing path sampling the same region we use events from Hindu Kush recorded at Canadian stations. Such a path has been used by Thomas et al. (2002) and Wookey and Kendall (2008) where they found reflections from D″ as well as anisotropy in both source–receiver combinations. Due to the limited number of deep Hindu Kush events and stations in Canada in a suitable epicentral distance the data quality and quantity for this direction is poorer than for the Kurile to Germany path.

We use vespagrams (see e.g. Rost and Thomas, 2002) to analyse the polarities of the seismic waves. Three examples for P-wave reflections are shown for the path Kuriles–Germany (Fig. 2a–c). In each vespagram the P and PcP waves are visible as well as PdP waves

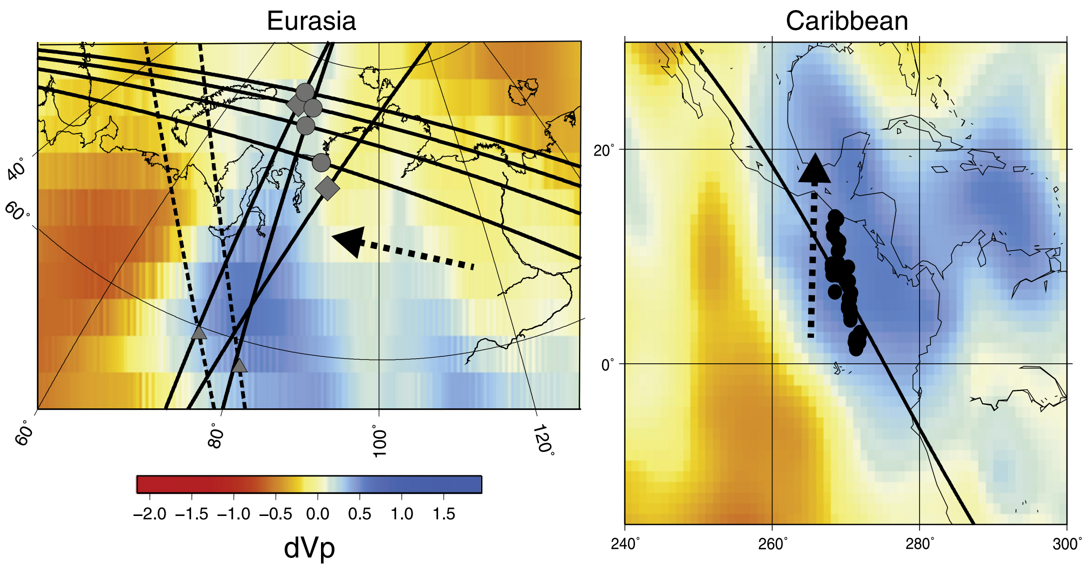

Fig. 1. a) The region imaged with sources in the Kuriles and Japan recorded in Germany (reflection points in the lowermost mantle shown as grey circles) and for the perpendicular raypath sources in the Hindu–Kush region and receivers in Canada (reflection points as grey diamonds). Additionally shown are source receiver combinations for which the great circle path crosses the region in other orientations (thick and thin dashed lines) with reflection points in the lowermost mantle shown as grey triangles. b) Earthquakes in South America recorded at stations in North America with reflection points in the lowermost mantle as black circles. The PcP and PdP reflection points for both regions lie in a fast velocity region for the model of Kárason and van der Hilst (2001). Dashed arrows show the paleosubduction direction 100 Ma ago of the Kula and Farallon plates, respectively.

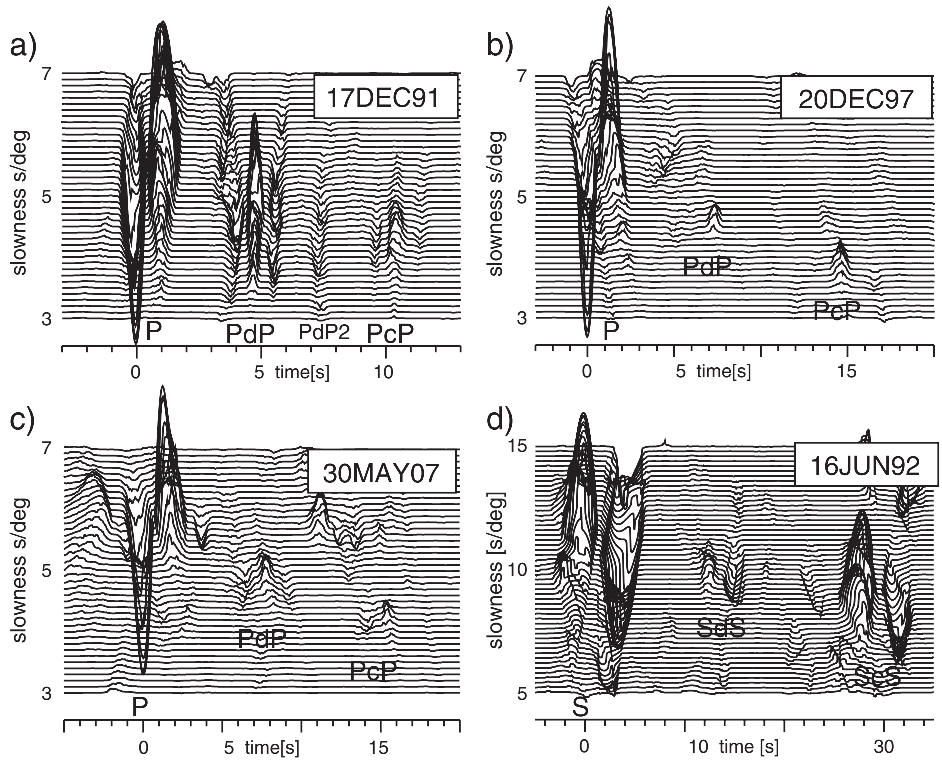

Fig. 2. Three examples of vespagrams containing PdP waves with the same polarity as P and PcP waves (a–c) and one example of an event containing SdS with the same polarity as S and ScS (d). The amplitudes of PdP are generally small except for the event 17 Dec 1991. Event 17 Dec 1991 also shows a possible second reflection between PdP and PcP, PdP2. The data in (a–c) are filtered with a bandpass filter 1 to 10 s order 2, the events containing SdS is filtered with a low pass filter of 3 s order 2 and the T-components are used.

with a slowness value and travel time between P and PcP. Inspecting the PcP and PdP waveforms and polarities, we find that in each case the PdP polarities are the same as the PcP polarities, i.e., differing from the observation in the Caribbean region. In the case of 17 Dec 1991, the P waveform is a two-lobed wavelet whereas the PcP and PdP wavelets are three-lobed. We also analyse the S-waves and polarities of SdS and ScS and find that the polarities of SdS are the same as the CMB reflection and the direct S-wave (Fig. 2d).

For the orthogonal path from the Hindu Kush to Canada the PdP polarity indicates a positive P-wave contrast across the D″ reflector (Fig. 3a). Due to the larger epicentral distance of this source–receiver combination (78°) the slowness values of P, PdP and PcP are not separated as much as for the perpendicular direction from the Kuriles to Germany. In addition, large multiples can be seen with P-slowness. Nevertheless the PdP waveform is the same as the PcP waveform. To verify the waveform for the North–South path, we re-analyse the data from Thomas et al. (2002) in terms of the polarities of the waves. The presence of a reflector was established using frequency–wavenumber analysis for the station INK by Thomas et al. (2002) even though the slowness resolution is poor for the source array vespagram. The data have been cross-correlated with the P-wavelet to account for differing source mechanisms (see Thomas et al., 2002). In the vespagram the polarity of the PdP wave is again the same as for the PcP wave.

In summary, we find that the polarity of S-wave reflectors at the top of D″ are always positive (i.e., SdS has the same polarity as ScS) in both regions, while the P-wave reflector is more complicated: under

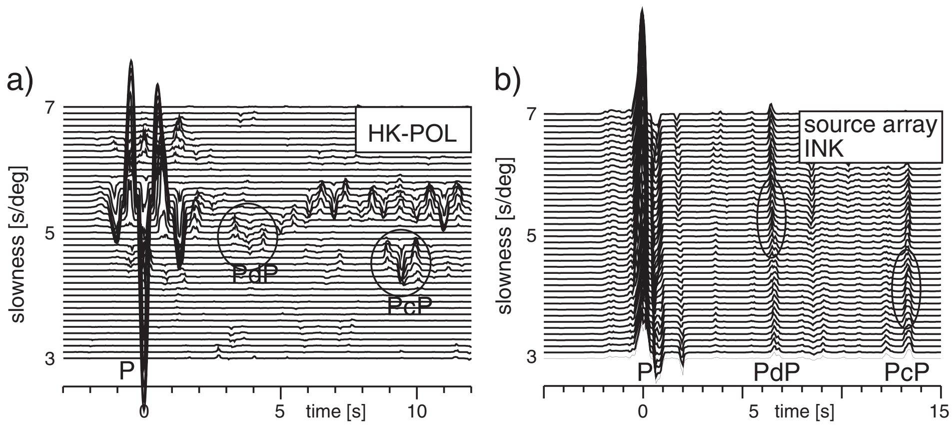

Fig. 3. Two events for the Hindu Kush to Canada path. a) Receiver array vespagram of a Hindu Kush event (25 Feb 2005) recorded at the POLARIS NWT stations. PdP with slowness between P and PcP shows the same waveform as PcP. Crustal reverberations can also be seen with a slowness close to P slowness. b) Source vespagram of Hindu–Kush events recorded at station INK. The data are from Thomas et al. (2002) where they showed with frequency–wavenumber analysis that the slowness of the phase interpreted as PdP lies between the P and PcP slowness. The slowness resolution in the vespagram here is poor due to the small aperture of the source array (the Hindu Kush events).

the Caribbean, the PdP polarity is negative whereas under Eurasia the PdP polarity is positive for two orthogonal paths. The difference in polarity of P-wave reflections at the CMB cannot be due to changes in focal mechanisms, since the P and PcP waves in general have the same polarity and the take off angle of PdP lies between P and PcP take off angles. We suggest, therefore, that the varying polarity of the P-wave reflector with azimuth is caused by anisotropy in D″.

3. Anisotropy calculations

To reconcile the differing observations in the two fast velocity regions in the lowermost mantle, we test different models of phase changes and anisotropy. Lay and Garnero (2007) indicate that anisotropic variations need to be considered to explain the available D″ observations, especially the observed velocity contrasts, something also inferred in earlier work on the basis of waveform modelling (Matzel et al., 1996). Ammann et al. (2010) show that a rapid change in anisotropy can explain sharp reflectors in D″ due to a strong crystallographic texture of post-perovskite. This offers an explanation for short period P-wave reflections despite the possibility of a large phase loop of perovskite to post-perovskite (Catalli et al., 2009). We follow the procedure outlined in Ammann et al. (2010) to try to explain the variations in reflection polarity in our observations. This procedure interpolates/extrapolates ab initio-calculated single crystal elasticities for perovskite and post-perovskite structured $MgSiO_3$ over pressure and temperature ranges appropriate to the lower 1000 km of the mantle, using gradients from Wentzcovitch et al. (2004, 2006). These functions are evaluated along an assumed geotherm (Stacey and Davies, 2004). In all models we assume a reflection at a nominal distance from an instantaneous change in material properties (either alignment, or crystal structure and alignment) 150 km above the CMB. Anisotropic models comprise 12% aligned single crystal elasticities in a linear mixture with their isotropic equivalent. Our anisotropic models assume that, for a given slip system, 12% of the grains are aligned with the slip plane parallel to the CMB and the slip direction in the direction of the flow. The models measure the variation in velocity perturbation and the reflection coefficients across the discontinuity with azimuth (i.e., with respect to the deformation slip direction). Since we observe the sign of this perturbation to vary in the data, an anisotropic model is required. Velocity is a function of both azimuth and angle of incidence in the orthorhombic models tested, so we choose the latter to be appropriate for comparison with S- and P-reflections at 75° epicentral distance.

We test two classes of models. The first is where the D″ discontinuity is solely a change in alignment of a single phase (as might be expected with a strong localisation of strain, Ammann et al., 2010). This is tested for both post-perovskite and perovskite for completeness. In the second class a phase transformation from perovskite to post-perovskite is also included. We test two slip systems for post-perovskite, [100](010) inferred from analogue studies using CaIrO3 (e.g., Walte et al., 2009; Yamazaki et al., 2006), and [100](001) which has recently been suggested by diamond anvil cell studies (Miyagi et al., 2010). For perovskite deformation we assume [010](100) (Mainprice et al., 2008). The elastic constants for each model tested here are given in Table 1.

Table 1
Elastic constants (C11 to C66) representing the lower layers of models a–e, and isotropic ppv and pv (upper layers). Elastic constants are in GPa, density (rho) is given in kg/m^3.

	PPV (iso)	PV (iso)	Model A	Model B	Model C	Model D	Model E
C11	1038	1035	1055	1057	1055	1055	1042
C12	450	473	443	442	451	451	475
C13	450	473	451	451	443	443	483
C22	1038	1035	1053	1055	1024	1024	1039
C23	450	473	455	456	455	455	470
C33	1038	1035	1024	1021	1053	1053	1022
C44	294	281	290	289	290	290	281
C55	294	281	301	302	287	287	280
C66	294	281	287	286	301	301	287
rho	5297	5232	5302	5302	5302	5302	5237

Fig. 4 shows the variation of P–P and SH–SH wave reflection coefficient as a function of azimuth for the different models tested. While the SV–SH reflection coefficient is potentially non-zero in anisotropic media, for the models presented here it is generally much smaller than the SH–SH reflection, which will dominate the amplitude observed on the transverse component. Only the case of a phase transformation and [100](010) alignment in post-perovskite appears to match the required periodicity in reflection coefficient and constant positive reflection coefficient in VS (Fig. 4b). The data therefore appear to be most consistent with this model; at least of those we have tested. The modelling we use is simplistic, and would be improved by adoption of a more realistic flow geometry and proper petrophysical calculation of post-perovskite texture. There is also currently rather a scarcity of calculated single crystal properties at lowermost mantle pressures and temperatures, particularly for perovskite. This potentially limits the accuracy of the extrapolation of the elasticities. These limitations notwithstanding, we suggest that these observations are consistent with reflections from a textured post-perovskite layer.

4. Discussion

Several hypotheses have been discussed recently that could cause the D″ layer and explain the seismic energy reflected from it. One of those is a subducted slab with and without phase transitions (Kendall, 2000; Kendall and Silver, 1998; Sidorin et al., 1999; Thomas et al., 2004b).

Subducted slabs without a phase transition cannot explain the reflections since the gradient of such a slab would be too large to generate high-frequency waves (Sidorin and Gurnis, 1998; Thomas et al., 2004a). Sidorin et al. (1999) postulated a phase transition in the lowermost mantle that seems to agree with the recently discovered post-perovskite phase transition (Murakami et al., 2004; Oganov and Ono, 2004). Since then much work has gone into determining the depth and Clapeyron slope of this phase transition (see, e.g., Hirose, 2007). The thickness of the transition zone between perovskite and post-perovskite is also a case for debate. Catalli et al. (2009) found a

Fig. 4. Predicted reflection coefficients of P- and S-waves as a function of azimuth for different modelled D″ discontinuities. These are calculated for PdP and SdS phases at 75° epicentral distance; the azimuth is measured relative to the slip direction (i.e., the direction of lowermost mantle flow, indicated by the arrow). The left and central panels show the changes in reflection coefficient of P–P and SH–SH respectively (black line) upon crossing a D″ discontinuity 150 km above the CMB. These come from elastic constants at lowermost mantle temperature and pressure conditions (see main text, Table 1 and Ammann et al. (2010) for details). The rightmost panels show the model assumed. a, c and e show cases where the discontinuity is only due to the imposition of anisotropy (either on a pure perovskite or post-perovskite lowermost mantle). Panels b and d also include the pv–ppv phase transformation. Two suggested slip systems for post-perovskite are tested (e.g., Miyagi et al., 2010; Walte et al., 2009; Yamazaki et al., 2006). The coloured spots around the periphery indicate the polarities measured from the data (C = Caribbean paths; E1, E2, E3 = Eurasian). The azimuths assigned to these are based on predictions of flow directions at the base of the mantle (Lithgow-Bertelloni and Richards, 1998). Blue and red spots indicate positive and negative polarities respectively. The only model tested which appears compatible with the data incorporates a pv–ppv phase change with a [100](010) texture in the lower layer. Other models either have incorrect periodicity in δVP (for example, the pure perovskite model), or do not show a consistent VSH increase (for example, the pure post-perovskite model). Dashed lines indicate where the reflection coefficient becomes critical and amplitude determination there is more difficult since a phase shift is imposed on the data.

large transition zone with a linear mixture of perovskite and post-perovskite for iron rich perovskite or perovskite with a low Si/Mg ratio. The resulting gradient would not be sufficiently sharp to explain the reflections seen with short-period P-wave data. But other studies find thicknesses of the transition that lie in the range of 90 to 120 km, which can be detected with seismic P-waves (e.g., Lay, 2008; Weber,

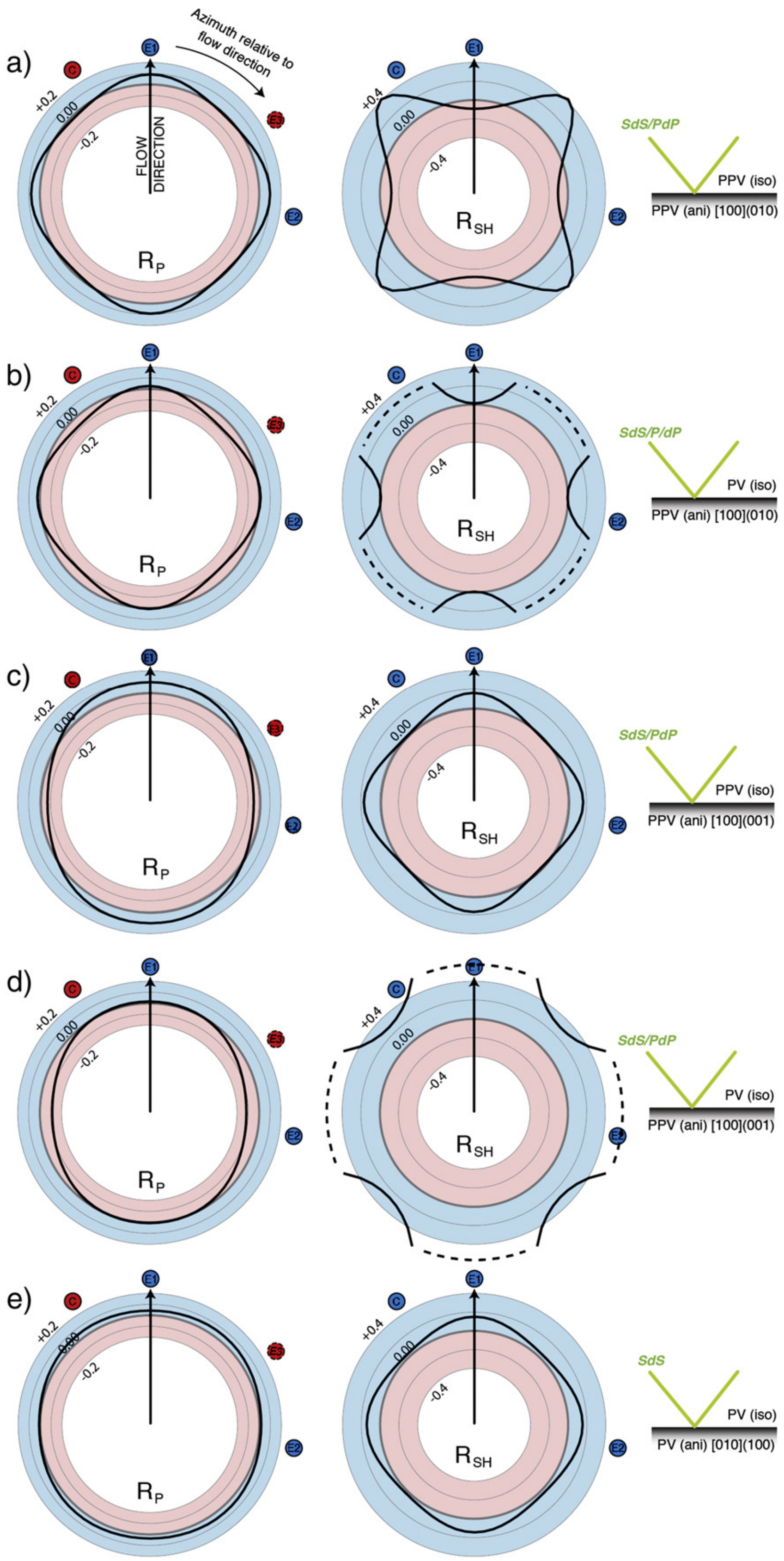

1993). In recent work, Ammann et al. (2010) present a mechanism that can produce sharper reflectors in the D″ region, i.e., a model that can explain short-period P-wave reflections at D″ structures.

Seismic anisotropy in the D″ region has been observed in both locations discussed here using S-wave splitting. Beneath the Caribbean, several studies find transverse isotropy (e.g. Kendall and Silver, 1996, Kendall and Silver, 1998; Moore et al., 2004; Lay et al., 1998). Recently, tilted anisotropy has been discussed here (Garnero et al., 2004; Maupin et al., 2005; Nowacki et al., 2010). In the region beneath Eurasia, both Thomas et al. (2002) and Wookey and Kendall (2008) find evidence for anisotropy.

We find two different scenarios for our two seismically fast regions: under the Caribbean the polarity of the PdP wave is opposite to the polarity of the PcP and P waves (Hutko et al., 2008; Kito et al., 2007), whereas the SdS polarity is the same as for the ScS and S wave polarity. These results indicate a positive S velocity jump and a negative P velocity jump across the discontinuity. For epicentral distances used here, the density changes have less impact on seismic waves than velocity contrasts (Lay and Garnero, 2007) and we therefore assume that the polarity is influenced mostly by the velocity rather than impedance. For the region beneath Eurasia on the other hand, the P and S-wave contrasts seem to be both positive, since PdP (SdS) has the same polarity as PcP (ScS) for two orthogonal directions. It would not be possible to explain these observations with a simple model of a post-perovskite phase transition as presented by Wookey et al. (2005b) due to the positive PdP polarities.

One obvious difference for those two regions is the travel path of the seismic waves with respect to the flow direction of the slab that is likely to be responsible for the fast velocities in the D″ region. The direction of subduction of palaeo slabs 80 to 100 Ma ago (Lithgow-Bertelloni and Richards, 1998) is indicated in Fig. 1 as dashed arrows. Assuming that the direction has not changed in the deep mantle the path for the South America to North America combination lies near 45° to the slab propagation direction. For the Kurile to Germany path the travel path is along the direction of slab (0°) flow and Hindu Kush events recorded in Canada travel perpendicular to the slab flow direction (90°).

Comparing our polarity results to the reflection coefficient model resulting from the anisotropy calculations, we find that the model with pure perovskite (i.e. no phase change) cannot explain our observations since all PdP-wave polarities should be the same as PcP (Fig. 4e). The model with post-perovskite and no phase transition can explain the P-wave observations for both regions but fails to explain overall positive S-wave contrasts (Fig. 4a). For the region beneath Eurasia a negative S-wave reflector would be expected which disagrees with the observations (see also Thomas et al., 2004a; Kito et al., 2007). Only the case with a phase transition and aligned post-perovskite (Fig. 4b) can explain all observations from both regions. For this case the SdS wave should have an increase in velocity in all regions but the PdP polarities differ for Eurasia and the Caribbean.

Another region beneath Southeast Asia shows reflections from a D″ structure, with small negative (around 1%) P-wave velocity contrasts and positive S-wave contrasts (Chaloner et al., 2009) and tilted anisotropy has been observed in the same region (Thomas et al., 2007). In this case a much more complicated subduction history prevails, with several subduction regions merging in the deep mantle beneath Southeast Asia (Lithgow-Bertelloni and Richards, 1998). It is therefore difficult to test our hypothesis on this additional example and it would be useful to study additional regions in the Earth using P and S-wave polarities of reflected waves at D″ structures and seismic anisotropy in D″.

The reflection coefficients of Fig. 4 could potentially provide amplitude constraints on the reflected waves. For instance, in model b a wave travelling in the flow direction should have a PdP amplitude smaller than for a wave travelling at 45° to the flow. We have measured amplitudes in our datasets but find strong variations in the PdP amplitudes: in the Caribbean region, the PdP reflection exhibits between 10 and 30% of the P amplitude whereas in the Eurasian region PdP shows between 10 and more than 100% of the P wave amplitude. Since the amplitude of a reflected wave can also vary strongly due to the topography of the reflector (Thomas and Weber, 1997) and velocity gradients (e.g., Lay, 2008) this measurement may not help to distinguish between different models indeed due to anisotropy it becomes even more complicated to use amplitude as a diagnostic tool. The use of stacking methods may distort the amplitude measurements but in most cases the relatively weak PdP phase cannot be identified without such stacking methods. Beneath Eurasia some of the raw seismograms show strong D″ reflections but even those are very variable (e.g., Lay, 2007; Thomas and Weber, 1997; Weber and Davis, 1990) and in several cases the D″ reflection cannot be identified without stacking.

In our case the polarities of the seismic waves clearly show a difference depending on which region the waves travel through. The P-wave polarities are an especially good diagnostic tool as S-wave polarities seem to be positive in all regions (i.e., the SdS wave has the same polarity as the ScS and S wave). One assumption for this model to work, however, is the direction of waves travelling with respect to the flow direction of the slab. We have used the data from Lithgow-Bertelloni and Richards (1998) from 100 Ma and have assumed that the direction of the slab in the deep mantle did not change much. It would be useful to have supporting observations that intersect the crossing paths (Fig. 1a) in a 45° direction. If this direction showed negative PdP polarities and positive SdS polarities, the assumption of the slab flow direction would be superfluous. We have been searching for such a crossing path. It turns out that the reflection points for potential additional paths are further to the Southwest or Southeast (see triangles in Fig. 1a). The reflection points to the Southeast from western Pacific events recorded at Spitsbergen station KBS show a strong Moho multiple at the arrival time of PdP in the data and can therefore not be used. However, an example for a Chinese earthquake recorded at Greenland stations HJO and DAG (Fig. 5 and thick dashed travel path in Fig. 1a) shows an arrival between P and PcP that indicates a negative polarity PdP. This wave cannot be the reflection of the Moho discontinuity, or the pP arrival, since the move-out changes with distance. We therefore assume that it is a reflection from D″. Unfortunately not enough stations are available to use array methods to fully establish the slowness and backazimuth of this wave. If this wave is indeed a D″ reflection it would support our model of an anisotropic region including a phase change

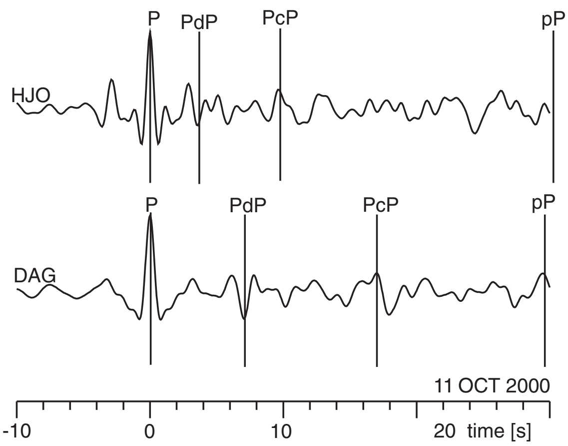

Fig. 5. Seismogram section of a source receiver combination with a great circle path that crosses the paths in Fig. 2 in approximately 45°. The reflection points are south of the ones for Hindu Kush–Japan and Kuriles–Germany (see also Fig. 1a). We show two stations for this combination of events in China and receivers in Greenland (HJO and DAG). The arrival times of PdP. PcP, P and pP are indicated. The traces have been cross correlated with the P wavelet and station DAG shows a clear negative polarity for PdP; the polarity at HJO is less unambiguous, but is not obviously positive.

without the assumption of slab flow direction in the lowermost mantle (see Fig. 4b).

5. Conclusion

Observations of polarities of reflected waves from D″ structures beneath the Caribbean in a high-velocity region indicate positive S-wave velocity contrast but a negative P-wave contrast. In a second high velocity region, beneath Eurasia, evidence for positive P- and S-wave contrasts is found for two perpendicular paths. To reconcile these differing observations in two fast velocity regions we test a model of anisotropy in the post-perovskite phase in D″. Our best fitting models include a phase change of perovskite to post-perovskite and a fraction of 12% alignment in the post-perovskite minerals. Depending on the angle of the ray crossing this region, we find negative or positive P-wave velocity jumps. The S-wave velocity jump is always positive, in agreement with the observations. One assumption for this hypothesis to work is the direction of slab flow in the lower mantle. In order to be independent of this, a path that crosses the other two perpendicular paths in 45° would have to show a negative P-wave contrast and positive S-wave contrast. We find evidence for such a case in P-waves which makes our preferred model a good explanation for the differing polarity observations.

Acknowledgments

We would like to thank the CNDC (Canadian National Data Centre) for providing events from Canadian stations and the Seismological Central Observatory Germany (SZO) for data from German stations. Data from Greenland were collected via the IRIS consortium, station DAG is run by GEOFON and Nat. Survey and Cadastre Denmark, station HJO was funded by NERC and Danish Lithosphere project. Maps were created with GMT (Wessel and Smith, 1991) and data were analysed with Seismic Handler (Stammler, 1993). Reviews by Thorne Lay and one anonymous reviewer helped to improve the manuscript.

References

Ammann, M.W., Brodholt, J.P., Wookey, J., Dobson, D.P., 2010. First-principles constraints on diffusion in lower-mantle minerals and a weak D '' layer. Nature 465, 462–465.
Bullen, K.E., 1949. Compressibility-pressure hypothesis and the Earth's interior. Mon. Not. R. Astron. Soc., Geophys. Suppl. 5, 355–368.
Catalli, K., Shim, S.H., Prakapenka, V., 2009. Thickness and Clapeyron slope of the post-perovskite boundary. Nature 462, 782–785.
Chaloner, J., Thomas, C., Rietbrock, A., 2009. P-and S-wave reflectors in D″ beneath South-East Asia. Geophys. J. Int. 179, 1080–1092.
Garnero, E.J., Revenaugh, J., Williams, Q., Lay, T., Kellogg, L.H., 1998. Ultralow velocity zones at the core-mantle boundary. In: Gurnis, M., Wysession, M., Knittle, E., Buffett, B.A. (Eds.), The Core Mantle Boundary Region. Geodyn. Series, 28. AGU, Washington D.C., USA, pp. 97–118.
Garnero, E.J., Maupin, V., Lay, T., Fouch, M.J., 2004. Variable azimuthal anisotropy in the Earth's lower mantle. Science 306, 259–261.
Grand, S.P., 2002. Mantle shear-wave tomography and the fate of subducted slabs. Philos. Trans. R. Soc. London, Ser. A 360, 2475–2491.
Hedlin, M.A.H., Shearer, P.M., Earle, P.S., 1997. Seismic evidence for small-scale heterogeneity throughout the Earth's mantle. Nature 387, 145–150.
Hernlund, J.W., Thomas, C., Tackley, P.J., 2005. A doubling of the post-perovskite phase boundary and the structure of the lowermost mantle. Nature 434, 882–886.
Hirose, K., 2007. Discovery of post-perovskite phase transition and the nature of D″ layer. In: Hirose, K., Brodholt, J., Lay, T., Yuen, D. (Eds.), Post-perovskite, the Last Mantle Phase Transition. American Geophysical Union, Washington D. C., USA, pp. 19–35.
Hutko, A., Lay, T., Revenaugh, J., Garnero, E.J., 2006. Seismic detection of folded, subducted lithosphere at the core-mantle boundary. Nature 441, 333–336.
Hutko, A.R., Lay, T., Revenaugh, J., Garnero, E.J., 2008. Anticorrelated seismic velocity anomalies from post-perovskite in the lowermost mantle. Science 320, 1070–1074.
Kárason, H., van der Hilst, R.D., 2001. Tomographic imaging of the lowermost mantle with differential times of refracted and diffracted core phases (PKP, Pdiff). J. Geophys. Res. 106, 6569–6587.
Kawai, K., Takeuchi, N., Geller, R.J., Fuji, N., 2007. Possible evidence for a double crossing phase transition in D″ beneath Central America from inversion of seismic waveforms. Geophys. Res. Lett. 34, L09314. doi:10.1029/2007GL029642.
Kendall, J.-M., 2000. Seismic Anisotropy in the boundary layers of the mantle. In: Karato, S., Forte, A., Lieberman, R., Masters, G., Stixrude, L. (Eds.), Earth's Deep Interior: Mineral Physics and Tomography From the Atomic to the Global Scale. : American Geophysical Union Geophysical Monograph, 117. American Geophysical Union, Washington D.C, pp. 133–159.
Kendall, J.M., Silver, P.G., 1996. Constraints from seismic anisotropy on the nature of the lowermost mantle. Nature 381, 409–412.
Kendall, J.-M., Shearer, P.M., 1994. Lateral variations in D″ thickness from long-period shear wave data. J. Geophys. Res. 99, 11575–11590.
Kendall, J.-M., Silver, P.G., 1998. Investigating causes of D″ anisotropy. In: Gurnis, M., Wysession, M., Knittle, E., Buffett, B.A. (Eds.), The Core Mantle Boundary Region. Geodyn. Series, 28. AGU, Washington D.C., USA, pp. 97–118.
Kito, T., Rost, S., Thomas, C., Garnero, E.J., 2007. New insights into the P- and S-wave velocity structure of the D″ discontinuity beneath the Cocos plate. Geophys. J. Int. 169, 1201–1209.
Lay, T., 2007. Deep earth structure — lower mantle and D". In: Romanowicz, B., Dziewonski, A. (Eds.), Treatise on Geophysics. Seismology and Structure of the Earth, Vol. 1. Elsevier, Amsterdam, pp. 619–654.
Lay, T., 2008. Sharpness of the D″ discontinuity beneath the Cocos Plate: implications for the perovskite to post-perovskite phase transition art-no: L03304 Geophys. Res. Lett. 35. doi:10.1029/2007GL032465.
Lay, T., Garnero, E.J., 2007. Reconciling the post-perovskite phase with seismological observations of lowermost mantle structure. In: Hirose, K., Brodholt, J., Lay, T., Yuen, D. (Eds.), Post-perovskite, the Last Mantle Phase Transition. American Geophysical Union, Washington D. C., USA, pp. 129–154.
Lay, T., Helmberger, D.V., 1983. A lower mantle S-wave triplication and the shear velocity structure of D. Geophys. J. R. Astron. Soc. 75, 799–837.
Lay, T., Williams, Q., Garnero, E.J., Kellogg, L., Wysession, M.E., 1998. Seismic wave anisotropy in the D″ region and its implications. In: Gurnis, M., Wysession, M.E., Knittle, E., Buffett, B.A. (Eds.), The Core–Mantle Boundary Region. American Geophysical Union, Washington D.C., USA, pp. 299–318.
Lay, T., Garnero, E.J., Williams, Q., 2004. Partial melting in a thermo-chemical boundary layer at the base of the mantle. Phys. Earth Planet. Inter. 146, 441–467.
Lay, T., Hernlund, J., Garnero, E.J., Thorne, M.S., 2006. A post-perovskite lens and D″ heat flux beneath the central Pacific. Science 314, 1272–1276.
Lithgow-Bertelloni, C., Richards, M.A., 1998. The dynamics of Cenozoic and Mesozoic plate motions. Rev. Geophys. 36, 27–78.
Mainprice, D., Tommasi, A., Ferre, D., Carrez, P., Cordier, P., 2008. Predicted glide systems and crystal preferred orientations of polycrystalline silicate Mg–Perovskite at high pressure: implications for the seismic anisotropy in the lower mantle. Earth Planet. Sci. Lett. 271, 135–144.
Masters, G., Laske, G., Bolton, H., Dziewonski, A.M., 2000. The relative behavior of shear velocity, bulk sound speed, and compressional velocity in the mantle: implications for chemical and thermal structure. In: Karato, S., Forte, A.M., Liebermann, R.C., Masters, G., Stixrude, L. (Eds.), Earth's Deep Interior: Mineral Physics and Tomography From the Atomic to the Global Scale. AGU, Washington, D.C, pp. 63–87.
Matzel, E., Sen, M.K., Grand, S.P., 1996. Evidence for anisotropy in the deep mantle beneath Alaska. Geophys. Res. Lett. 23, 2417–2420.
Maupin, V., Garnero, E.J., Lay, T., Fouch, M.J., 2005. Azimuthal anisotropy in the D″ layer beneath the Caribbean. J. Geophys. Res. 110, 8301.
Merkel, S., Kubo, A., Miyagi, L., Speziale, S., Duffy, T.S., Mao, H.-K., Wenk, H.-R., 2006. Plastic deformation of MgGeO3 post-perovskite at lower mantle pressures. Science 311, 644–646.
Miyagi, L., Kanitpanyacharoen, W., Kaercher, P., Lee, K.K.M., Wenk, H.R., 2010. Slip systems in MgSiO3 post-perovskite: implications for D″ anisotropy. Science 329, 1639–1641.
Moore, M., Garnero, E.J., Lay, T., Williams, Q., 2004. Synthesizing shear wave splitting and waveform complexity for lowermost mantle structures with low-velocity lamellae and transverse isotropy. J. Geophys. Res. 109, B02319. doi:10.1029/2003JB002546.
Murakami, M., Hirose, K., Sata, N., Ohishi, Y., Kawamura, K., 2004. Phase transition of MgSiO3 perovskite in the deep lower mantle. Science 304, 855–858.
Murakami, M., Sinogeikin, S.V., Bass, J.D., Sata, N., Ohishi, Y., Hirose, K., 2007. Sound velocity of MgSiO3 post-perovskite phase: A Constraint on the D″ discontinuity. Earth Planet. Sci. Lett. 259, 18–23.
Nowacki, A., Wookey, J., Kendall, J.-M., 2010. Deformation of the lowermost mantle from seismic anisotropy. Nature 467, 1091–1094.
Oganov, A.R., Ono, S., 2004. Theoretical and experimental evidence for a post-perovskite phase of MgSiO3 in Earth's D″ layer. Nature 430, 445–448.
Oganov, A.R., Martonak, R., Laio, A., Raiteri, P., Parrinello, M., 2005. Anisotropy of Earth's D″ layer and stacking faults in the $MgSiO_3$ post-perovskite phase. Nature 438, 1142–1144.
Ohta, K., Hirose, K., Lay, T., Sata, N., Ohishi, Y., 2008. Phase transitions in pyrolite and MORB at lowermost mantle conditions: implications for a MORB-rich pile above the core–mantle boundary. *Earth Planet.* Sci. Lett. 267, 107–117.
Pulliam, J., Sen, M.K., 1998. Seismic anisotropy in the core–mantle transition zone. Geophys. J. Int. 135, 113–128.
Ritsema, J., Van Heijst, H.J., 2000. Seismic imaging of structural heterogeneity in Earth's mantle: evidence for large-scale mantle flow. Sci. Prog. 83 (1), 925.
Rokosky, J.M., Lay, T., Garnero, E.J., 2006. High-resolution investigation of shear wave anisotropy in D″ beneath the Cocos Plate. Earth Planet. Sci. Lett. 248, 411–425.
Rost, S., Revenaugh, J., 2003. Small-scale ultralow-velocity zone structure imaged by ScP. J. Geophys. Res. 108, 2056. doi:10.1029/2001JB001627.
Rost, S., Thomas, C., 2002. Array seismology: methods and applications. Rev. Geophys. 40. doi:10.1029/2000RG000100.
Sidorin, I., Gurnis, M., 1998. Geodynamically consistent seismic velocity predictions at the base of the mantle. In: Gurnis, M., Wysession, M.E., Knittle, E., Buffett, B.A. (Eds.), The Core–Mantle Boundary Region. American Geophysical Union, Washington D.C., USA, pp. 209–230.

Sidorin, I., Gurnis, M., Helmberger, D.V., 1999. Dynamics of a phase change at the base of the mantle consistent with seismological observations. J. Geophys. Res. 104, 15005–15023.
Stacey, F.D., Davies, P.M., 2004. High pressure equations of state with applications to the lower mantle and core. Phys. Earth Planet. Inter. 142, 137–184.
Stackhouse, S., Brodholt, J.P., 2007. The high temperature elasticity of MgSiO3 post-perovskite. In: Hirose, K., Brodholt, J., Lay, T., Yuen, D. (Eds.), Post-perovskite, the Last Mantle Phase Transition. American Geophysical Union, Washington D. C., USA, pp. 99–114.
Stammler, K., 1993. Seismic Handler — programmable multichannel data handler for interactive and automatic processing of seismological analysis. Comput. Geosci. 19, 135–140.
Tan, E., Gurnis, M., Han, L.J., 2002. Slabs in the lower mantle and their modulation of plume formation. Geochem. Geophys. Geosyst. 3. doi:10.1029/2001GC000238 art-no:1067.
Thomas, C., Weber, M., 1997. P-velocity heterogeneities in the lower mantle determined with the German Regional Seismic Network: improvement of previous models and results of 2D modelling. Phys. Earth Planet. Inter. 101, 105–117.
Thomas, C., Weber, M., Wicks, C.W., Scherbaum, F., 1999. Small scatterers in the lower mantle observed at German broadband arrays. J. Geophys. Res. 104, 15073–15088.
Thomas, C., Kendall, J.-M., Weber, M., 2002. The lowermost mantle beneath northern Asia: (1) multi-azimuth studies of heterogeneity. Geophys. J. Int. 151, 279–295.
Thomas, C., Garnero, E.J., Lay, T., 2004a. High-resolution imaging of lowermost mantle structure under the Cocos Plate. J. Geophys. Res. 109. doi:10.1029/2004JB003013.
Thomas, C., Kendall, J.-M., Lowman, J., 2004b. Lower mantle seismic discontinuities and the thermal morphology of subducted slabs. *Earth Planet.* Sci. Lett. 255, 105–113.
Thomas, C., Wookey, J., Simpson, M.R., 2007. D″ anisotropy beneath Southeast Asia. Geophys. Res. Lett. 4, L04301. doi:10.1029/2006GL028965.
Tsuchiya, T., Tsuchiya, J., Umemoto, K., Wentzcovitch, R.M., 2004. Phase transition in MgSiO3 perovskite in the earth's lower mantle. *Earth Planet.* Sci. Lett. 224, 241–248.
van der Hilst, R.D., de Hoop, M.V., Wang, P., Shim, S.H., Ma, P., Tenorio, L., 2007. Seismostratigraphy and thermal structure of Earth's core–mantle boundary region. Science 315, 1813–1817.
Vidale, J.E., Hedlin, M.A.H., 1998. Evidence for partial melt at the core mantle boundary north of Tonga from the strong scattering of seismic waves. Nature 391, 682–685.
Walte, N.P., Heidelbach, F., Miyajima, N., Frost, D.J., Rubie, D.C., Dobson, D.P., 2009. Transformation textures in post-perovskite: understanding mantle flow in the D″ layer of the Earth. Geophys. Res. Lett. 36. doi:10.1029/2008GL036840 Art no: L04302.
Weber, M., 1993. P- and S-wave reflections from anomalies in the lowermost mantle. Geophys. J. Int. 115, 183–210.
Weber, M., Davis, J.P., 1990. Evidence of a laterally variable lower mantle structure from P- and S waves. Geophys. J. Int. 102, 231–255.
Wentzcovitch, R.M., Karki, B.B., Cococcioni, M., de Gironcoli, S., 2004. Thermoelastic properties of MgSiO3-perovskite: insights on the nature of the Earth's lower mantle. Phys. Rev. Lett. 92 Art no: 018501.
Wentzcovitch, R.M., Tsuchiya, T., Tsuchiya, J., 2006. MgSiO3 post-perovskite at D″ conditions. Proc. Natl. Acad. Sci. U.S.A. 103, 543–546.
Wessel, P., Smith, W.H.F., 1991. Free software helps map and display data. Eos Trans. AGU 72 (441), 445–446.
Wookey, J., Kendall, J.M., 2008. Constraints on lowermost mantle mineralogy and fabric beneath Siberia from seismic anisotropy. *Earth Planet.* Sci. Lett. 275, 32–42.
Wookey, J., Kendall, J.-M., Rümpker, G., 2005a. Lowermost mantle anisotropy beneath the north Pacific from differential S–ScS splitting. Geophys. J. Int. 161, 829–838.
Wookey, J., Stackhouse, S., Kendall, J.M., Brodholt, J.P., Price, G.D., 2005b. Efficacy of the post-perovskite phase as an explanation of lowermost mantle seismic properties. Nature 438, 1004–1008.
Wysession, M.E., Lay, T., Revenaugh, J., Williams, Q., Garnero, E.J., Jeanloz, R., Kellogg, L., 1998. The D″ discontinuity and its implications. In: Gurnis, M., Wysession, M.E., Knittle, E., Buffett, B.A. (Eds.), The Core–Mantle Boundary Region. American Geophysical Union, Washington D.C., USA, pp. 273–298.
Yamazaki, D., Karato, S.-I., 2007. Lattice-preferred orientation of lower mantle materials and seismic anisotropy in the D″ layer. In: Hirose, K., Brodholt, J., Lay, T., Yuen, D. (Eds.), Post-perovskite, the Last Mantle Phase Transition. American Geophysical Union, Washington D.C., USA, pp. 69–78.
Yamazaki, D., Yoshino, T., Ohfuji, H., Ando, J.I., Yoneda, A., 2006. Origin of seismic anisotropy in the D″ layer inferred from shear deformation experiments on post-perovskite phase. Earth Planet. Sci. Lett. 252, 372–378.